Research question: “How does the Angle of Attack of a Frisbee disc and the velocity of airflow over it affect the generated lift force?” - Physics Extended Essay

Word count: 3978

Contents:

1. Introduction

This investigation is inspired by the sport Ultimate Frisbee and the disc used in it. When an object travels through air, 4 major forces will act on the object *(NASA.gov)*. These forces are: Thrust, Drag, Lift, Weight *(Figure 1.1)*. Of the 4 forces, lift is "the force that directly opposes the weight of an [object] and holds the [object] in the air" *(NASA Glenn Research Center)*. For this research paper, only the lift force of the frisbee disc will be investigated.

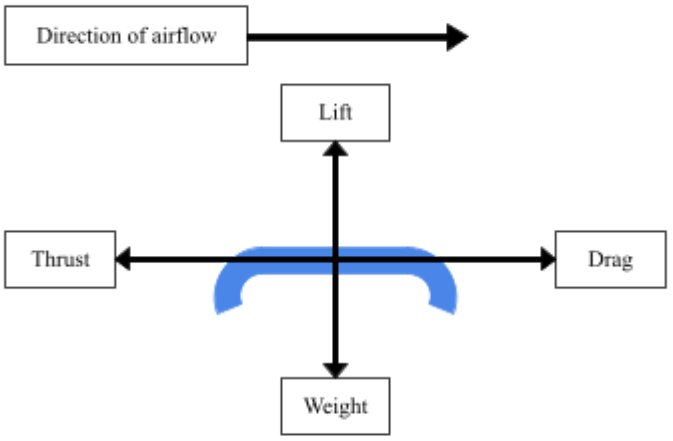

Figure 1.1: Free-Body Diagram of the 4 forces of a frisbee travelling through air.

Any object that produces lift and drag when moved through air is called an aerofoil *(Britannica)*, which tends to be optimized to generate a large lift force while generating a small induced drag force. Aerofoils come in various shapes and sizes, and a frisbee disc is a type of an aerofoil. With proper techniques, the throw of a frisbee can make the frisbee glide relatively long distances due to its generated lift force. These techniques mostly aim to optimize two variables of the frisbee's flight: angle of attack and velocity. Therefore, the aim of this research paper is to investigate **how the angle of attack along with the velocity of airflow over a frisbee disc affects the generated lift force** with the intent to optimize Ultimate Frisbee..

2. Theory of Investigation

2.1. Attributes of Aerofoils:

An aerofoil has 3 major attributes that determines its generated lift force in an airflow of constant velocity and air density: Angle of Attack (θ, measured in °) - defined as "the angle formed by the Chord of the aerofoil and the direction of the relative wind" *(SKYbrary.aero)*, Camber - defined as "an imaginary line which lies halfway between the upper surface and lower surface of the airfoil and intersects the chord line at the leading and trailing edges" *(NASA Glenn Research Center)*, and Shape. This is illustrated in *Figure 2.1* below for both a conventional aerofoil and a frisbee.

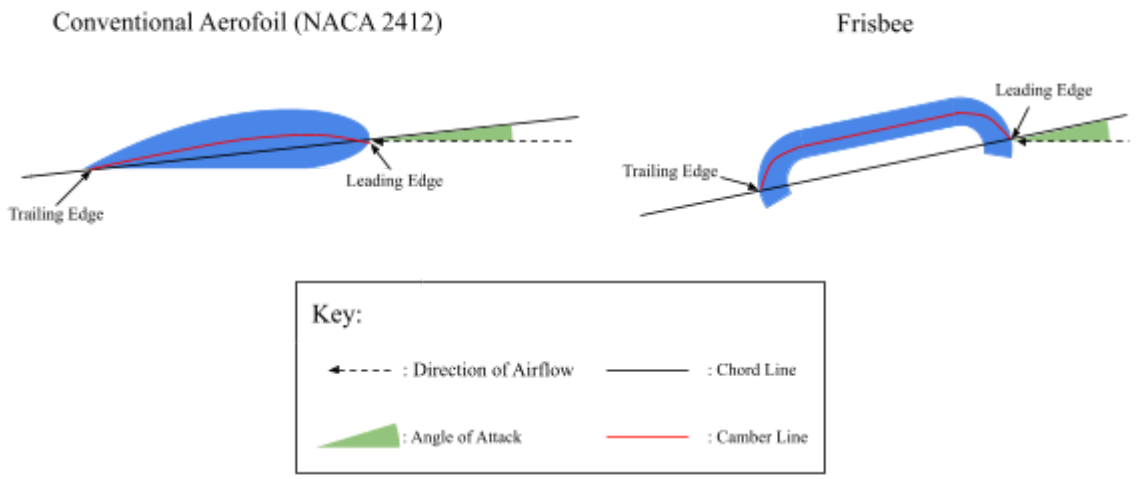

Figure 2.1: Labelled Diagram of a Conventional Aerofoil and of a Frisbee

2.2. How an Aerofoil generates Lift:

There are 2 theories explaining how lift force is generated in air. One of them uses Newton's Third Law, and the other one uses Bernoulli's Principle.

2.2.1. Theory using Newton's Laws of Motion:

Newton's Third Law states that "Whenever one object exerts a force on another object, the second object exerts an equal and opposite on the first" *(NASA Glenn Research Center)*. An aerofoil at flight will collide into air molecules. If an aerofoil has a positive angle of attack, the collision will cause air molecules at the lower surface to deflect downwards, causing a change in momentum. Using Newton's Third Law, the force caused by the change in vertical momentum that the aerofoil exerts on air molecules will cause air molecules to exert a force on the aerofoil that is equal in magnitude upwards, resulting in lift. *(Figure 2.2)*

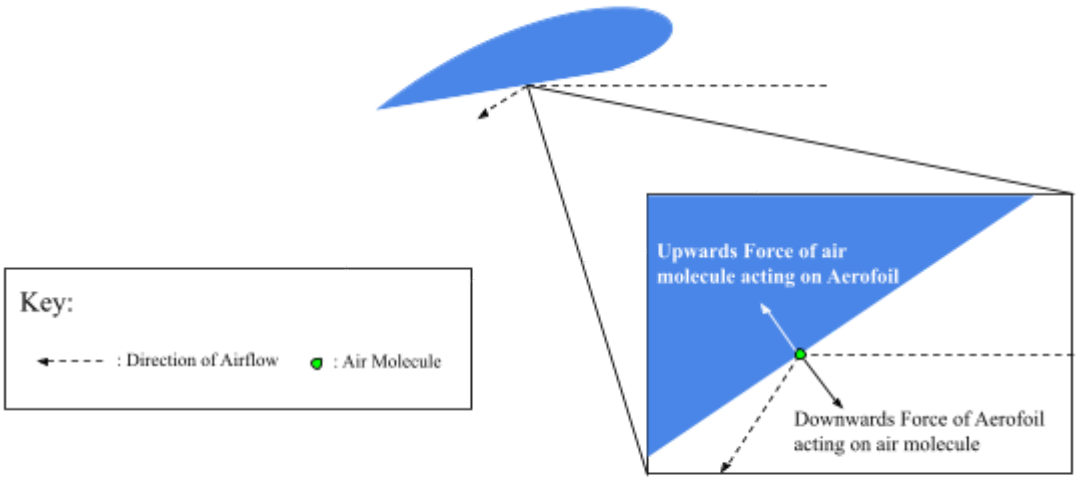

Figure 2.2: Magnified Diagram of Theory of Lift using Newton's Third law

2.2.2. Theory using Bernoulli's Principle:

Bernoulli's Principle, states that "an increase in velocity leads to a decrease in pressure" *(Massachusetts Institute of Technology)*, expressed as:

$$p + \frac{1}{2}\rho v^2 + \rho g h = Constant \text{ [1]},$$

where:

- p is the Static Fluid Pressure, measured in Pa,
- $\frac{1}{2}\rho v^2$ is the Dynamic Fluid Pressure, measured in Jm^{-3}, in which:
    - ρ is the Fluid Density, measured in kgm^{-3},
    - v is the Velocity of Flow, measured in ms^{-1},
- g is the acceleration of free fall, measured in ms^{-2}
- h is the height of elevation of the flow, measured in m
    - In the context of Aerodynamics, the change in height of airflow around an aerofoil is negligible, therefore assumed constant.

assuming no heat transfer, no work done by the fluid, and incompressible flow.

When the velocity of airflow is being measured at different regions of an aerofoil with a positive camber and angle of attack, the results will display that the upper surface's velocity of airflow is faster than that of the lower surface *(Figure 2.3)*. Using Bernoulli's Principle [1], a negative correlation between p and v^2 can be observed[1]. This means that pressure at the top of the aerofoil will be smaller

[1] Assuming incompressible flow, meaning that ρ is taken as a constant. This will be further discussed in **3. Variables and Measurements.**

than that at the bottom of the aerofoil, which results in a pressure gradient, generating lift on the aerofoil.

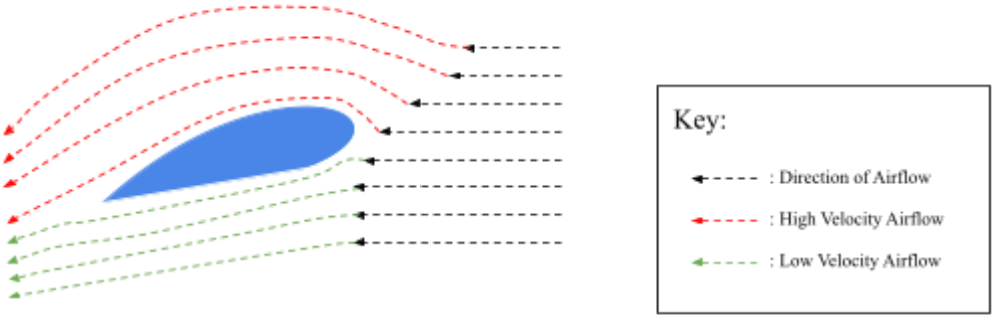

Figure 2.3: Velocity of Airflow around an Aerofoil

2.2.3. Validity of Both Theories:

Although arguments are made about which theory out of the two makes a better explanation for how lift is generated, both are correct and obey the physics principles as "The Bernoulli equation is simply a statement of the principle of conservation of energy in fluids [while] Conservation of momentum and Newton's 3rd law are equally valid as foundation principles of nature" *(R. Nave)*.

2.3. Relating Lift to Angle of Attack and Velocity of Airflow:

A method to calculate lift is using the Lift Equation, which states that:

$$F = C_L \times S \times \frac{1}{2}\rho v^2 \text{ [2]},$$

where:

- F is the generated Lift Force, measured in N,
- C_L is the Coefficient of Lift (C_L), no units,

- S is the Wing Surface Area, measured in m^2,
- ρ is the Air Density, measured in kgm^{-3},
- v is the Velocity of Airflow, measured in ms^{-1}.

2.3.1. Mathematical Interpretation

As the forces acting on an aerofoil are caused by a change in vertical momentum by air molecules, Newton's Second Law can be applied:

$$F_{Total} = \frac{d\,mv}{d\,t} \text{ [3]},$$

where:

- F_{Total} is the total Resultant Force on an aerofoil, measured in N,
- m is mass, measures in kg,
- v is the Velocity of Airflow, measured in ms^{-1},
- t is time, measured in s.

By integrating [3] and using steps [3.1] to [3.5], equation [4] can be obtained:

$$\int F_{Total}\,dt = \int \frac{d\,mv}{dt}\,dt \text{ [3.1]}$$

$$F_{total}t = mv \text{ [3.2]}$$

$$F_{Total} = v\frac{m}{t} \text{ [3.3]}$$

When Angle of Attack and shape of aerofoil is constant, $F_{Total} \propto F_{Lift}$. Hence:

$$F_{Lift} = Cv\frac{m}{t} \text{ [4]},$$

where C is a constant.

For a moving fluid, the rate of change of mass of air molecules can be determined using mass flow rate ($\dot{m}$, measured in kgs^{-1}). For a fluid flowing at constant velocity, mass flow rate is determined using:

$$\dot{m} = \frac{m}{t} \text{ [5]},$$

which can be mathematically related to v and ρ by using [5.1]:

$$\dot{m} = \rho A v \text{ [5.1]},$$

where A is the Cross-Sectional Area over which the air flows, measured in m^2.

For a controlled value of surface area, shape, and angle of attack of an aerofoil, A is a constant.

Substituting [5] and [5.1] into [4], it can be deduced that:

$$F_{Lift} = 2 \times CA \times \frac{1}{2}\rho v^2 \text{ [6]},$$

where CA is a constant, measured in m^2.

Therefore, the relationship $F \propto \rho v^2$ and $F \propto A$ can be reasonably concluded.

$\frac{1}{2}$ is multiplied to ρv^2 in [6] and the Lift Equation [2] as $\frac{1}{2}\rho v^2$ is the dynamic pressure of an airflow, appearing in Bernoulli's Principle [1].

In the context of this paper, the constant $2 \times CA$ will be affected by the planform area of the wing *(Figure 2.4)*, the shape of the aerofoil, and the angle of attack. In the Lift Equation, this constant is represented by $S \times C_L$.

Using $F \propto A$, it can be reasonably concluded that $F \propto S$ is also true. C_L encapsulates both the shape of the aerofoil and the angle of attack as quantifying these variables involves various complications.

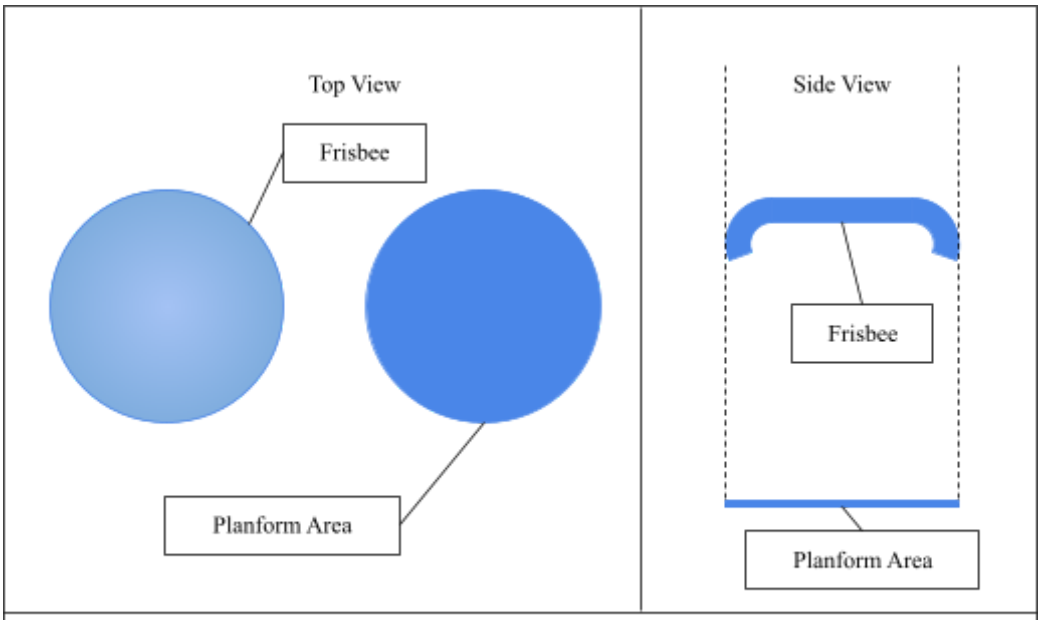

Figure 2.4: 2D Diagram illustrating the Planform Area of a Frisbee.

2.4. Hypotheses:

2.4.1. Hypothesis for Velocity (v) and Lift (F):

Using the Lift Equation, it can be hypothesized that a proportionality can be observed between v^2 and F. To test this hypothesis, F will be measured for a range of values of v, and a graph will be plotted between v^2 and F to observe whether the relationship $F \propto v^2$ is satisfied.

2.4.2. Hypothesis for Angle of Attack (θ) and Lift (*F*):

In an Ultimate Frisbee game, a frisbee is optimally thrown at an angle of $10° \sim 20°$ *(University of Melbourne)*. This is due to the maximum lift-to-drag ratio for a flying disc is around $15°$ *(Scodary, 2007)*. Therefore, angle of attacks beyond $\pm 20°$ is beyond the scope of this investigation as the primary purpose of this investigation is for Ultimate Frisbee.

For a hypothetical flat aerofoil, an increase in θ will lead to more air molecules colliding with the frisbee, resulting in an increase in mass flow rate ($\dot{m}$) of air onto the aerofoil's surface *(Figure 2.5)*. Furthermore, for small values of θ ($-20° < \theta < 20°$), an increase in θ will result in an increase in the vertical component of the force of air molecules acting on the aerofoil (Refer back to *Figure 2.2*).

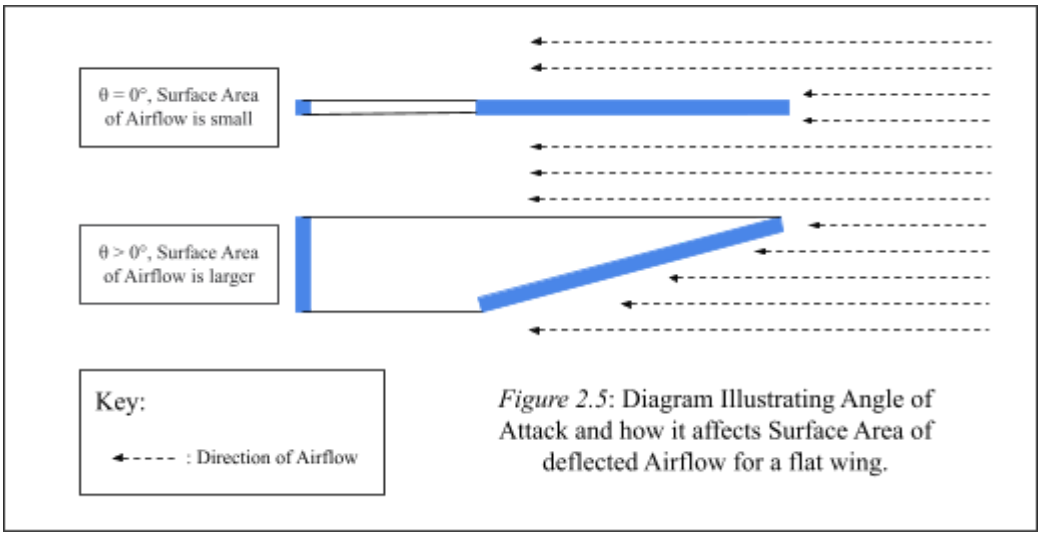

Figure 2.5: Diagram Illustrating Angle of Attack and how it affects Surface Area of deflected Airflow for a flat wing.

Since a frisbee disc that is similar to but not exactly a flat aerofoil due to its positive camber line *(Refer back to Figure 2.1.)*, it can be reasonably hypothesized that a positive correlation can be observed between between θ and *F* but not direct proportionality.

Past literature data on the lift coefficient of frisbee shows that a linear correlation exists between θ and C_L with a positive y-intercept ($0° < \theta < 30°$) *(Figure 2.6) (Potts and Crowther, 2005)*. Since the Lift Equation states that $F \propto C_L$, a linear relationship with a positive y-intercept can be hypothesized for θ and F, supporting my hypothesis.

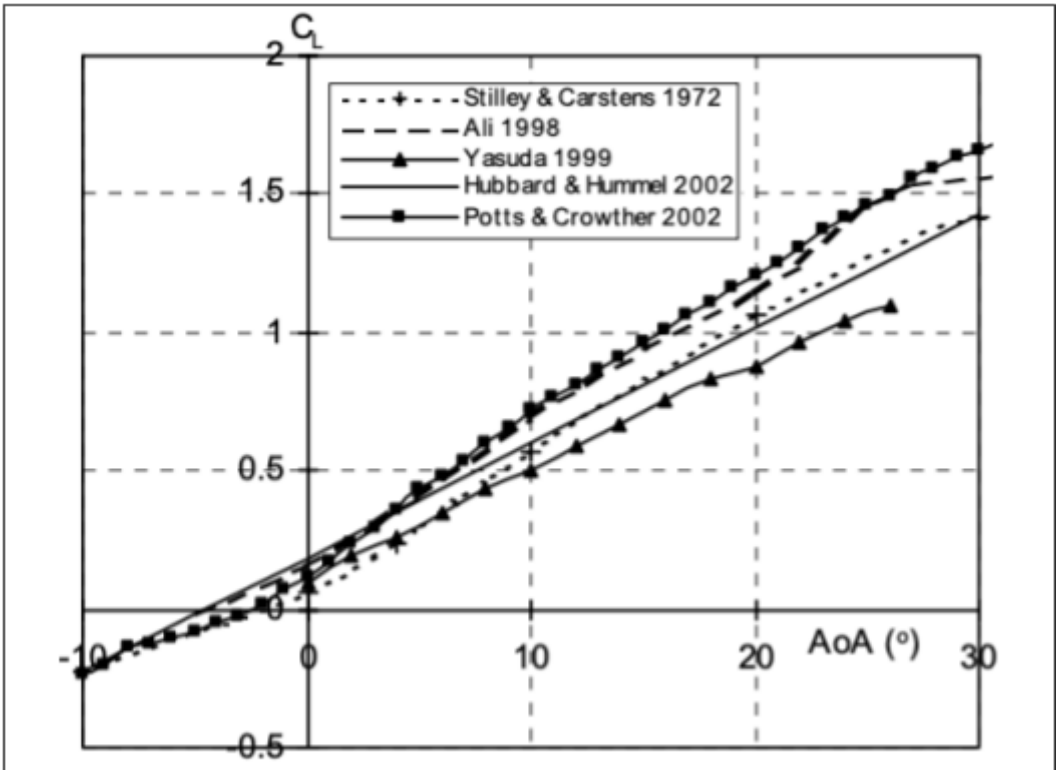

Figure 2.6: Potts, J., & Crowther, W. J. (2005). Comparison of the present experimental data to Frisbee-like circular planform wings from the literature - Lift Coefficient [Graph]. https://www.researchgate.net/publication/268559957_FrisbeeTM_Aerodynamics

3. Variables and Measurements

3.1. Velocity of Airflow (v/ms^{-1}):

This will be an Independent Variable when investigating relationship between F and v. v will be changed by using a fan with variable settings of wind speed $v = 0\, ms^{-1} \sim 4.68\, ms^{-1}$ [2]. This will be controlled by placing the frisbee disc inside a sealed wind tunnel, maximizing laminar flow and ensuring conservation of mass. If the frisbee disc is placed outside of the wind tunnel instead of within, using Bernoulli's Principle [1], the airflow that exits the wind tunnel will have a lower pressure than its surrounding air with no velocity. To balance out the pressure gradient, airflow will start to disperse, and result in turbulence *(Figure 3.1)*.

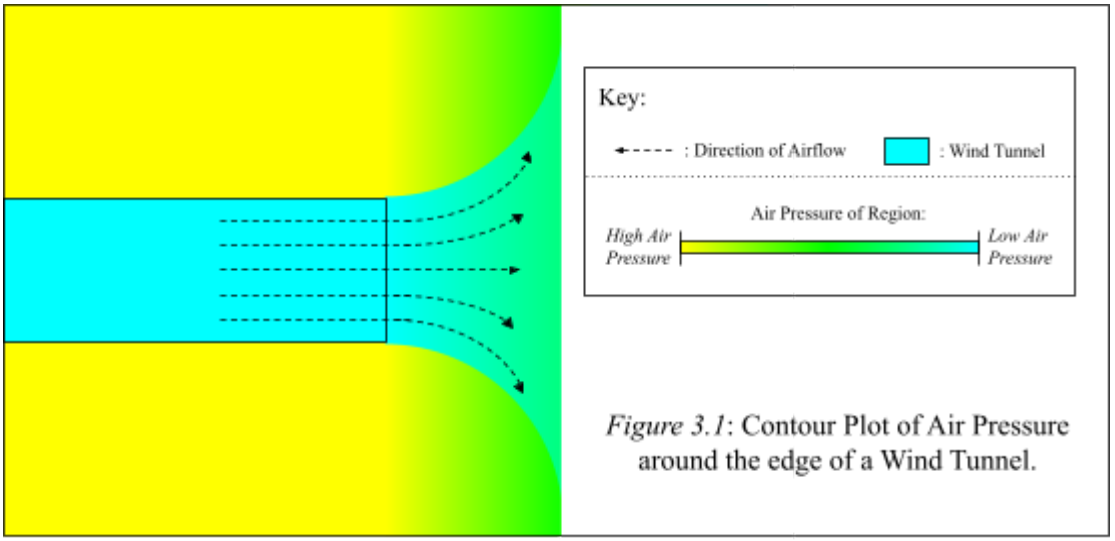

Figure 3.1: Contour Plot of Air Pressure around the edge of a Wind Tunnel.

7 varied settings of v (excluding $v = 0\, ms^{-1}$) wind speed will be tested using an anemometer across the wind tunnel and the average will be taken as the final wind speed for each reading. When investigating the relationship between θ and F, v will be controlled at $4.00\, ms^{-1}$.

[2] Domain obtained from maximum and minimum fan setting in Preliminary Trial.

3.2. Angle of Attack of Frisbee ($\theta/°$):

This will be an Independent Variable when investigating relationship between F and θ. This will be changed by fixing a rod on the bottom of the frisbee and using a clamp stand and clamp to stabilize the frisbee. The clamp will be rotated at different angles to produce varied angle configurations of $\theta = -18° \sim 18°$ [3]. By varying the increment for each value of θ by 2°, 19 values of θ can be obtained. When investigating the relationship between v and F, θ will be controlled at $\theta = 18°$.[4]

To ensure high precision and accuracy of the angle of attack of the frisbee disc relative to the air flow, an Inclinometer will be put against the top flat surface of the frisbee disc to measure its angle of incline, which is parallel to the chord line (See *Figure 2.1)*. Then, the Inclinometer will be put on the top surface of the wind tunnel to measure its angle of incline. If not 0°, then the jack used to support the wind tunnel will be adjusted to ensure that the incline of the wind tunnel, and hence the airflow, is at 0°. If this is not controlled, then the airflow created may be at an incline or decline, causing the measured angle of attack of the frisbee relative to the airflow to not be its true value.

3.3. Lift Force generated by Frisbee (F/N)

This will be measured by putting the clamp stand with the frisbee onto a weighing scale. Lift will be calculated by finding the difference between the total mass before and after having airflow, and then convert the mass difference from g to N. To improve precision, video recordings of the masses read by the weighing scales will be used. The recording will run for 10 seconds, 5 random readings will be taken throughout the video. Furthermore, 5 trials will be performed for each combination of v and θ. This means there should be $5 \times 5 \times 7 = 175$ data points for v and F and $5 \times 5 \times 19 = 475$ data points for θ and F.

---

[3] See 2.4.2

[4] In a preliminary trial, this produced the largest range of lift force for a given angle of attack.

3.4. Controlled Variables:

3.4.1. Planform Area (S) and Shape of Frisbee Disc:

This is controlled by using an Ultimate Frisbee Disc approved by the World Flying Disc Federation, which will be Discraft Ultrastar Web Mold. This has to be controlled as varying discs may result in changing both the shape and the Planform Area of the wing, causing inconsistent measurement of F. Diameter of Frisbee Disc measures out to be $27.31\ cm \pm 0.01\ cm$ using a Vernier Caliper, and is verified using Discraft's official dimensions of $27.305\ cm$ ($10.75''$). As the planform area of a Frisbee Disc is circular, it can be calculated using $S = (0.27305\ m)^2 \times \pi = 0.058556\ m^2$.

3.4.2. Air Density of Environment (ρ)

Air Density is calculated using the formula: $\rho = \frac{p}{RT}$ *(ChemEurope.com)*, where:

- p is the air pressure of the environment, measured in Pa
- R is the specific gas constant of air, measured in $Jkg^{-1}K^{-1}$
- T is the temperature of the environment, measured in K.

This can be controlled by performing the experiment:

- at constant pressure ($p = 101325\ Pa$) at sea level
- at a constant temperature ($T = 297.0\ K \pm 0.5\ K$) in an air-conditioned room.
- in dry air to control specific gas constant of air ($R = 287.05\ Jkg^{-1}K^{-1}$), where dehumidification settings are enabled with the air-conditioner.

- Increasing air humidity results in a decrease in R as the relative molecular mass of water vapor ($18.02\ gmol^{-1}$) is lower than that of dry air ($28.97\ gmol^{-1}$). At $298.0\ K$, 100% humid air will have air-to-water mass ratio of $1:0.019826$ (*EngineeringToolBox.com)*, which calculates to a maximum percentage discrepancy of 0.730%[5].

Thus, the calculated value of ρ is $\frac{101325\ Pa}{287.05\ Jkg^{-1}K^{-1} \times 297.0K} = 1.189\ kgm^{-3}$.

The uncertainty of ρ can be calculated as shown below:

$\%\ Uncertainty\ of\ \rho = \%\ Uncertainty\ of\ T + 0.730\%$ $= \frac{\pm 0.5K}{297.0K} \times 100\% + 0.730\%$ $= \pm 0.898\%$	$Absolute\ Uncertainty\ of\ \rho$ $= 1.189\ kgm^{-3} \times \pm 0.898\%$ $= \pm 0.011\ kgm^{-3}$

To ensure the controllability of ρ, however, requires the flow of fluid to be incompressible. A fluid's compressibility is determined by its Mach, which is calculated using:

$$M = \frac{u}{c}\ [7]\ \textit{(Labidi, 2019)},$$

where:

- M is the Mach Number, no units,
- u is the velocity of the fluid, measured in ms^{-1},
- c is the speed of sound in the fluid, measured in ms^{-1}.
    - In air at $297.0\ K$, the speed of sound is approximately $330\ ms^{-1}$

[5] See Appendix A for calculations.

By using [7], the maximum Mach of air for this investigation will be $\frac{4.68\ ms^{-1}}{330\ ms^{-1}} = 0.014$. Since air is considered incompressible when the Mach Number is below 0.3 *(Labidi, 2019)*, ρ can be considered as a constant.

4. Experimental Setup

4.1. 2D Diagram:

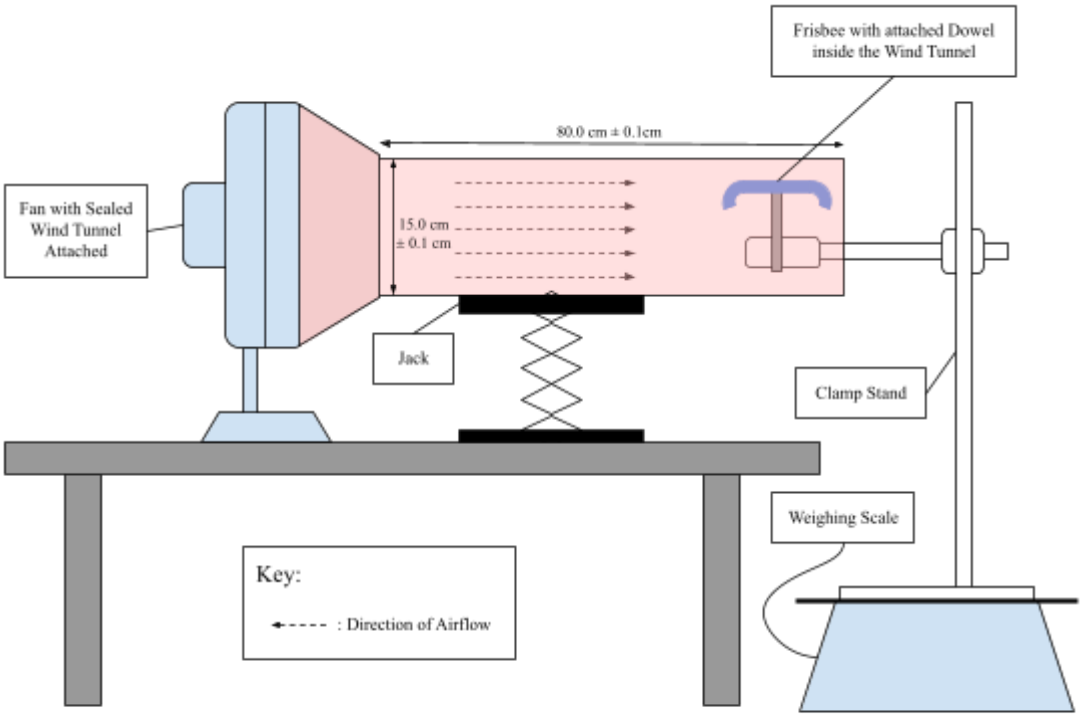

Figure 4.1: Simplified 2D Diagram of Experiment Setup with Key Dimensions

4.2. Apparatus List:

Table 1: Apparatus list for Experiment Setup in *Figure 4.1*.
Apparatus (Quantity: 1)
Fan (KDK) with Sealed Wind Tunnel Attached
Jack
Weighing Scale (OHAUS Pioneer™ Precision PX4202) ± 0.01g
Frisbee (Discraft Ultrastar Web Mold) with attached Dowel
Clamp Stand
Anemometer (Vernier) ± 0.01ms^{-1}
Inclinometer (No Brand) ± 1°

5. Data Collection and Data Processing

5.1. Relationship 1: Velocity of Airflow and Lift Force:

Table 2: Processed Data Table for How Velocity of Airflow affects Lift Force generated by a Frisbee[6]

Average Wind Speed, v/ms^{-1}	Uncertainty of v/ms^{-1}	v^2/m^2s^{-2}	Uncertainty of v^2/m^2s^{-2}	Interquartile Mean[7] Lift Force Generated by Frisbee, F/N	Uncertainty of F/N	% Uncertainty of F
4.19	0.07	17.36	0.56	0.364	0.008	2.25
3.68	0.12	13.69	0.86	0.263	0.008	3.05
3.33	0.03	11.11	0.22	0.202	0.007	3.62
2.45	0.07	6.08	0.33	0.126	0.016	12.7
3.00	0.07	9.00	0.40	0.174	0.008	4.70
4.01	0.07	16.00	0.53	0.323	0.008	2.34
1.96	0.05	3.87	0.20	0.049	0.018	37.4

$Constant$: $\theta = 18° \pm 0.5°$

5.1.1 Calculations for First Row: $v = 4.2\ ms^{-1}$

$\%\ Uncertainty\ of\ v = \frac{\pm 0.07\ ms^{-1}}{4.19\ ms^{-2}} \times 100\%$

$= \pm 1.60\%$ **(3sf)**

$\%\ Uncertainty\ of\ v^2 = \pm 1.60\% \times 2$

$= \pm 3.20\%$ **(3sf)**

$Absolute\ Uncertainty\ of\ v^2 = \pm 3.20\% \times 17.36\ ms^{-1}$

$= \pm 0.56\ ms^{-1}$ **(2dp)**

$Absolute\ Uncertainty\ of\ F = (3rd\ Quartile\ Mass - 1st\ Quartile\ Mass) \div 2 \times \frac{9.81N}{1000g}$

$= (2406.99g - 2405.32\ g) \div 2 \times \frac{9.81N}{1000g}$

$= 0.008\ N$

$\%\ Uncertainty\ of F = \frac{\pm 0.008N}{0.364N} \times 100\%$

$= \pm 2.25\%$ **(3sf)**

[6] See Appendix B for Raw Data

[7] Interquartile Mean is the mean of a data set excluding the largest 25% and smallest 25% of data. This is used to overcome the instability of lift when not rotating.

5.1.2. Graph:

Figure 5.1: Graph for how the square of Velocity of Airflow affects Lift Force generated by a Frisbee.

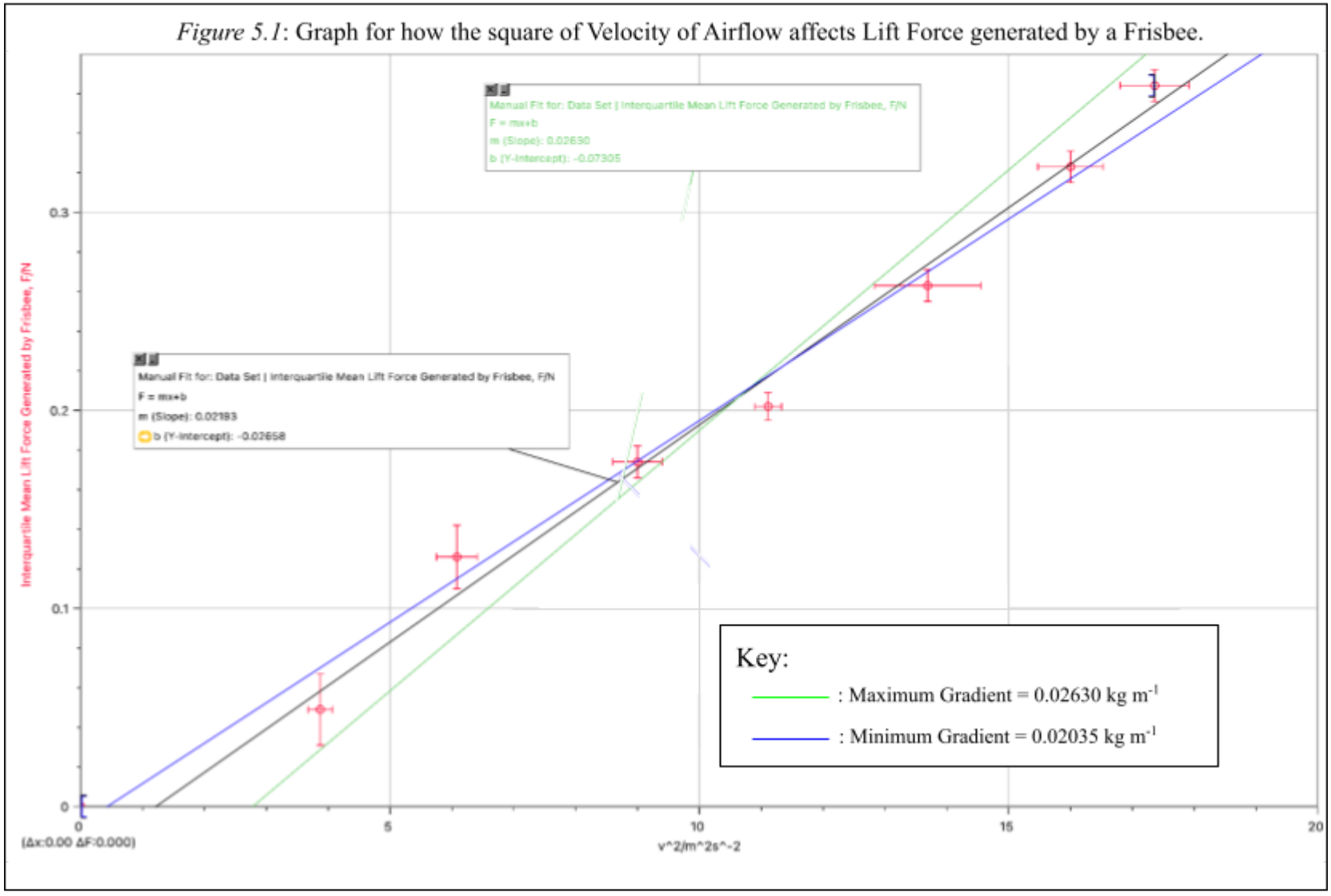

5.1.3. Graphical Calculation:

Table 3: Calculation for Gradient and Coefficient of Friction using *Figure 5.1*

Calculation for Gradient	***Calculation for C_L at $\theta = 18°$***
$Gradient = 0.2193\ kgm^{-1}$ $Gradient\ Range = 0.02630\ kgm^{-1} - 0.02035\ kgm^{-1}$ $= 0.00595\ kgm^{-1}$ $Gradient\ Uncertainty = 0.00595\ kgm^{-1} \div 2$ $= \pm 0.0030\ kgm^{-1}$ **(2sf rounded up)** $\%\ Uncertainty = \frac{\pm 0.0030\ kgm^{-1}}{0.02193\ kgm^{-1}} \times 100\%$ $= \pm 13.7\%$ $\therefore Gradient = 0.0219 kgm^{-1} \pm 0.0030\ kgm^{-1}$	$Gradient = \frac{F}{v^2} = \frac{C_L A\rho}{2}$ $\therefore C_L = \frac{2 \times Gradient}{A\rho}$ $\therefore C_L = \frac{2 \times 0.0219\ kgm^{-1}}{A\rho}$ $A = 0.058556\ m^2, \rho = 1.189\ kgm^{-3} \pm 0.011\ kgm^{-3}$ $\therefore C_L = \frac{2 \times 0.0219\ kgm^{-1}}{0.058556\ m^2 \times 1.189\ kgm^{-3}}$ $= 0.630$
Uncertainty of C_L at $\theta = 18°$	
$C_L = \frac{2 \times Gradient}{A\rho}$ $\%\ Uncertainty\ of\ Gradient = \pm 13.7\%$ $\%\ Uncertainty\ of\ \rho = \pm 0.898\%$	$\therefore \%\ Uncertainty\ of\ C_L = 0.898\% + 13.7\%$ $= \pm 14.6\%$ **(3sf)** $\therefore Absolute\ Uncertainty\ of\ C_L = 0.629 \times \pm 14.6\%$ $= \pm 0.15$ **(2sf rounded up)**
$\therefore C_L(18°) = 0.63 \pm 0.15.$	

5.2. Relationship 2: Angle of Attack and Lift Force:

Table 4: Processed Data Table for How Angle of Attack affects Lift Force generated by a Frisbee[8]				
Angle of Attack, $\theta/° \pm 0.5°$	% Uncertainty of θ	Interquartile Mean Lift Force Generated by Frisbee, F/N	Uncertainty of F/N	% Uncertainty of F
-18.0	2.78	-0.101	0.008	7.91
-16.0	3.13	-0.088	0.003	3.25
-14.0	3.57	-0.079	0.008	9.90
-12.0	4.17	-0.064	0.008	12.7
-10.0	5.00	-0.039	0.009	24.2
-8.0	6.25	-0.031	0.007	24.0
-6.0	8.33	-0.005	0.013	259
-4.0	12.5	0.015	0.009	56.6
-2.0	25.0	0.041	0.007	16.0
0.0	-	0.062	0.008	12.4
2.0	25.0	0.089	0.011	12.6
4.0	12.5	0.115	0.012	10.1
6.0	8.33	0.144	0.016	11.0
8.0	6.25	0.174	0.010	5.59
10.0	5.00	0.201	0.013	6.24
12.0	4.17	0.226	0.015	6.65
14.0	3.57	0.249	0.013	5.16
16.0	3.13	0.292	0.013	4.61
18.0	2.78	0.323	0.016	4.89

$Constant\text{: } v = 4.00\, ms^{-1} \pm 0.06\, ms^{-1}$

5.2.1 Calculations for First Row: $\theta = -18° \pm 0.5°$

$\%\ Uncertainty\ of\ \theta = \frac{\pm 0.5°}{-18°} \times 100\%$

$= \pm 2.78\%$ **(3sf)**

$Absolute\ Uncertainty\ of\ F = (3rd\ Quartile\ Mass - 1st\ Quartile\ Mass) \div 2 \times \frac{9.81N}{1000g}$

$= 0.008\ N$

$\%\ Uncertainty\ of F = \frac{\pm 0.008N}{-0.101N} \times 100\% = \pm 7.91\%$ **(3sf)**

[8] See Appendix C for Raw Data

5.2.2. Graph:

Figure 5.2: Graph for How Angle of Attack affects Lift Force generated by a Frisbee

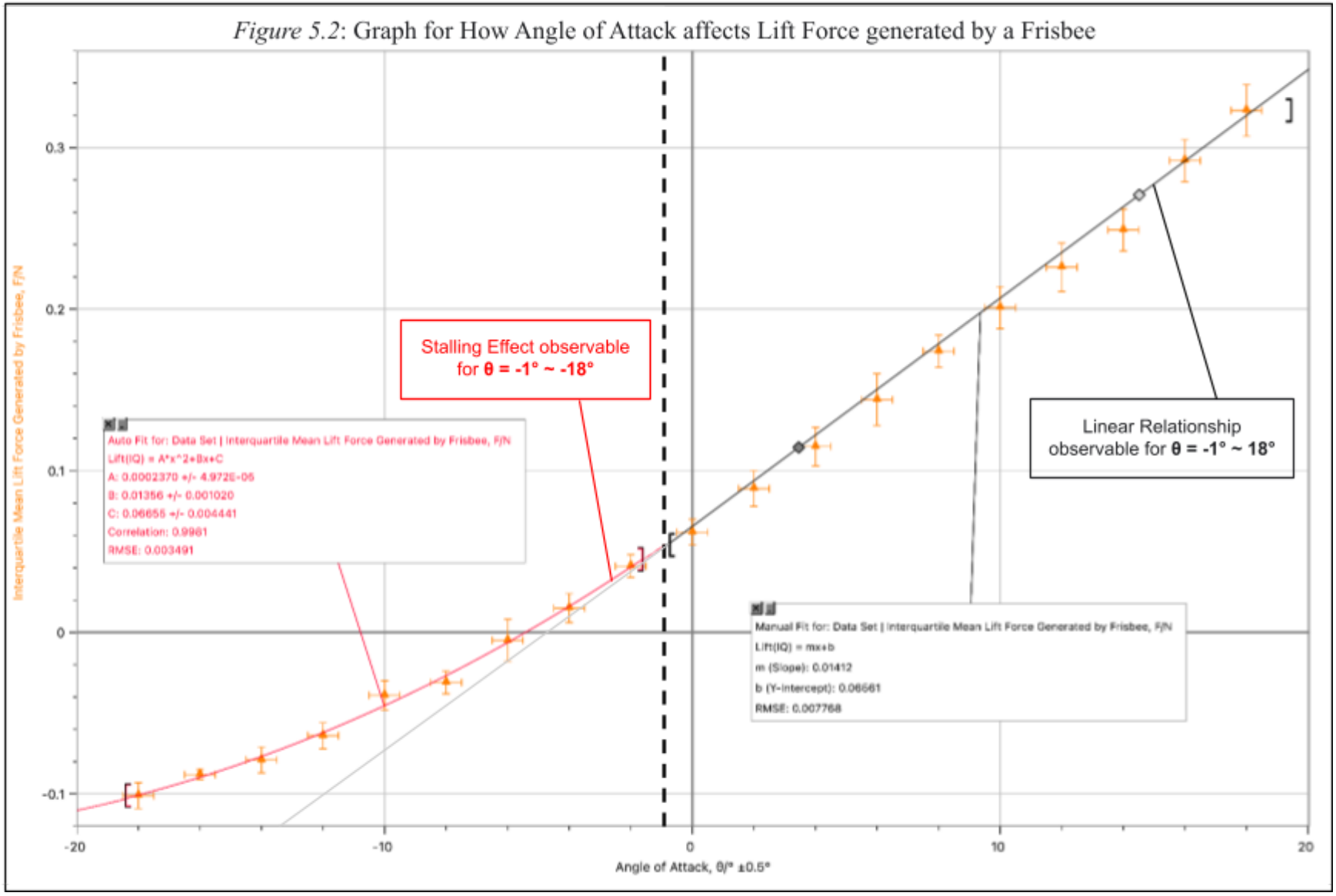

Graphical Calculation:

Table 5: Calculation for Gradient and Coefficient of Friction using *Figure 5.2*

Calculation for C_L ***at*** $\theta = 18°$	***Uncertainty of*** C_L ***at*** $\theta = 18°$
$A = 0.058556\,m^2, \rho = 1.189\,kgm^{-3} \pm 0.011\,kgm^{-3},$ $v = 4.00\,ms^{-1} \pm 0.06\,ms^{-1},\ F = 0.323\,N \pm 0.016\,N$ $F = C_L \times A \times \frac{1}{2}\rho \times v^2$ $\therefore C_L = \frac{2F}{A\rho v^2}$ $= \frac{2 \times 0.323\,N}{0.058556\,m^2 \times 1.189\,kgm^{-3} \times (4.00\,ms^{-1})^2}$ $= 0.580$	$C_L = \frac{2F}{A\rho v^2}$ $\%\ Uncertainty\ of\ F = \pm 4.89\%$ $\%\ Uncertainty\ of\ \rho = \pm 0.898\%$ $\%\ Uncertainty\ of\ v = \frac{\pm 0.06\,ms^{-1}}{4.00\,ms^{-1}} \times 100\% = 1.50\%$ $\%\ Uncertainty\ of\ C_L = 4.89\% + 0.898\% + 2 \times 1.50\%$ $= \pm 8.79\%$ **(3sf)** $\therefore Absolute\ Uncertainty\ of\ C_L = 0.580 \times \pm 8.79\%$ $= \pm 0.05$ **(1sf rounded up)** $\therefore C_L(18°) = 0.58 \pm 0.05.$
Calculation for C_L ***at*** $\theta = 0°$	***Uncertainty of*** C_L ***at*** $\theta = 0°$
$A = 0.058556\,m^2, \rho = 1.189\,kgm^{-3} \pm 0.011\,kgm^{-3},$ $v = 4.00\,ms^{-1} \pm 0.06\,ms^{-1},\ F = 0.062\,N \pm 0.008\,N$ $F = C_L \times A \times \frac{1}{2}\rho \times v^2$ $\therefore C_L = \frac{2F}{A\rho v^2}$ $= \frac{2 \times 0.062\,N}{0.058556\,m^2 \times 1.189\,kgm^{-3} \times (4.00\,ms^{-1})^2}$ $= 0.111$	$C_L = \frac{2F}{A\rho v^2}$ $\%\ Uncertainty\ of\ F = \pm 12.4\%$ $\%\ Uncertainty\ of\ \rho = \pm 0.168\%$ $\%\ Uncertainty\ of\ v = \frac{\pm 0.06\,ms^{-1}}{4.00\,ms^{-1}} \times 100\% = 1.50\%$ $\%\ Uncertainty\ of\ C_L = 12.4\% + 0.898\% + 2 \times 1.50\%$ $= \pm 16.3\%$ **(3sf)** $\therefore Absolute\ Uncertainty\ of\ C_L = 0.111 \times \pm 16.3\%$ $= \pm 0.02$ **(1sf rounded up)** $\therefore C_L(0°) = 0.11 \pm 0.02.$

5.3. Data and Graph Analysis:

5.3.1. Relationship 1: Velocity of Airflow and Lift Force:

The hypothesis predicts that "a proportionality can be observed between v^2 and F" *(2.4.1.)*. As shown in *Figure 5.1*, a linear relationship can be observed between v^2 and F, which demonstrates the validity of the hypothesis and the Lift Equation [2]. The line of best fit also goes through almost all error bars,

displaying the linear relationship hypothesized in 2.4.1. The one data point $v^2 = 11.11ms^{-1}$ is very close to the line of best fit, thus considered non-anomalous.

The y-intercept slightly deviates from the origin at -0.02658, It's small enough for $v^2 \propto F$ to hold true. However, since the gradient range doesn't include the origin, sources of systematic error are likely to be present.

5.3.2. Relationship 2: Angle of Attack and Lift Force:

The hypothesis predicts that a positive correlation will be exhibited between θ and *F* (See 2.4.2.). As shown in *Figure 5.2*, For $\theta = -1° \sim 18°$, the relationship observed is positive linear with no stalling; the linear line of best fit goes through all error bars of the data points in that range. This is consistent with the hypothesized relationship, as it states that a positive linear relationship is expected between θ and *F*. Furthermore, the line of best fit has a clear y-intercept greater than 0, which suggests that $\theta \propto F$ is not valid.

However, for $\theta = -18° \sim -1°$, a decreases in the gradient is observed as θ decreases, suggesting the presence of lift stalling. Although not hypothesized, this relationship is not unexpected as a frisbee disc is not a vertically symmetrical aerofoil shape. Furthermore, it can be concluded that for $\theta < -1°$, as θ becomes more negative, the rate of change of lift on a frisbee decreases. The data spread for θ and *F* is wide enough to observe a clear data trend. Considering the context of Ultimate Frisbee, $\theta = -18° \sim 18°$ is a large enough sample and range.

6. Conclusion and Evaluation

6.1. Comparison of Data from Relationships 1 and 2:

The calculated value of C_L for $\theta = 18°$ from Relationships 1 (0.63 ± 0.15) and 2 (0.58 ± 0.05) have a relatively high precision, with a percentage uncertainty of 14.6% and 8.79% respectively and are both within each other's uncertainty range. Since the data from both experiments agree with each other, a multivariable regression can be created between v^2, θ, and F to predict F for any given pair of θ and v, where $0\ m^2s^{-2} < v^2 < 17.36\ m^2s^{-2}$ and $-18° \leq \theta \leq 18°$. Therefore, using the regressions plotted in *Figure 5.1* and *5.2*, the relationship between v^2, θ, and F is:

$$F = 3.11 \times f(v^2) \times g(\theta)$$ [8][9], where

$$f(v^2) = 0.02193v^2 - 0.02658$$ [8.1] (See Section 5.1. and *Figure 5.1*)

$$g(\theta) = \begin{cases} 0.01412\,\theta + 0.06561, -1 < \theta \leq 18 \\ 0.000237\,\theta^2 + 0.01356\,\theta + 0.06655, -18 \leq \theta \leq -1 \end{cases}$$ [8.2] (See Section 5.2. and *Figure 5.2*),

which is shown in *Figure 5.3*[10] below, illustrating the value of F for any given combination of v^2 and θ. Hence, using *Figure 5.3*, we can conclude that:

- For all positive values of $f(v^2)$ in the range of $0\ ms^{-1} < v < 4.68\ ms^{-1}$, θ and F has a positive correlation. (Negative values of $f(v^2)$ are not considered as it is most likely caused by systematic errors.)
- For $g(\theta) \geq 0$, v^2 and F has a positive correlation, while for $g(\theta) < 0$, v^2 and F has a negative correlation.

[9] See Appendix D for derivation of regression.
[10] See Appendix E for Python Code used to create the plot.

Figure 5.3: 4 Perspectives of 3D Regression of Square of Velocity, Angle of Attack, and Lift using Figure 5.1 and 5.2

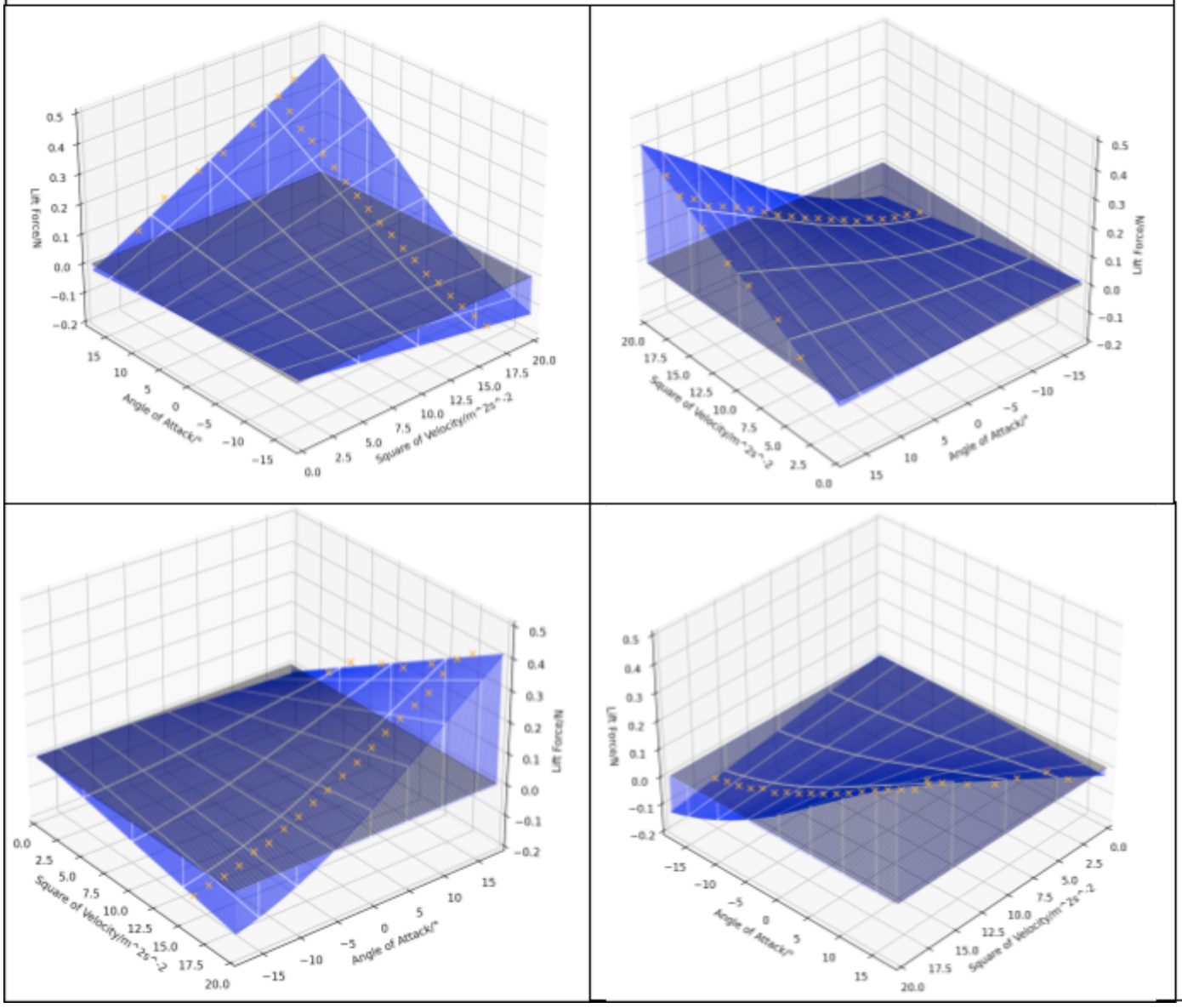

Key:

: Data from *Table 2* and *Table 4*

: $F = 3.11f(\mathbf{v}^2)g(\boldsymbol{\theta})$

6.2. Precision and Accuracy of Calculated Values:

Precision of C_L (0°) ***for*** θ ***and*** F***:***

$\%\ Uncertainty\ of\ C_L\ (0°) = \pm 16.3\%$

Percentage uncertainty within the range of 15% ~ 30%. However, considering C_L (0°) being a small value to begin with of 0.11 and how the absolute uncertainty of C_L (0°) is already very small, at $\pm\ 0.02$, I would consider C_L (0°) to be precise to an acceptable degree.

Accuracy of C_L (0°) ***for*** θ ***and*** F***:*** $C_L\ (0°) = 0.11 \pm 0.02$

There is no exact value for C_L (0°), however, a similar previously-performed experiment in better-controlled environments can be used to check the accuracy of results:

Literature Value *(Potts and Crowther, 2002)*: $C_L\ (0°) = 0.13$

$\%\ Discrepancy\ of\ C_L\ (0°) = \frac{0.11-0.13}{0.13} \times 100\% = -\ 15.4\%$

Discrepancy within the accepted range of uncertainty of $\pm$ 16.6%. Other sources gave results ranging from 0.1 to 0.2. Therefore, I would consider C_L (0°) as accurate to an acceptable degree.

6.3. Random Error, Systematic Error and Improvements:

6.3.1. Random Error

1. Uncertainty of measured F

$Max.\ Uncertainty\ for\ v\ and\ F = \pm 0.018.$

$Max.\ Uncertainty\ for\ \theta\ and\ F = \pm 0.016.$

This uncertainty is mainly due to the fluctuation of readings on the weighing scale when recording data, which was caused by the instability of flight of a stationary frisbee and the turbulence of airflow due to imperfect wind tunnel. In the data processing, Measures were taken to mitigate this effect by only taking the interquartile mean of the data as the final value. However, this still can be further

improved by attaching the frisbee to a motor to increase its gyroscopic effects, thus improving stability of flight *(N. Landell-Mills)*.

2. Uncertainty of measured v

$$Max.\ \%Uncertainty = \frac{\pm 0.07\ ms^{-1}}{2.45\ ms^{-1}} \times 100\% = \pm 2.70\%$$

This uncertainty is mainly caused by the fluctuation of readings of wind speed, suggesting inconsistent airflow. A method to improve this is to do what I did with measuring F, where I take a large quantity of trials (eg. 15) and only use the values within the interquartile range. Alternatively, using a more consistent and powerful fan may also lead to more precise data.

3. Uncertainty of measured θ

$$Uncertainty = \pm 0.5°$$

This uncertainty is mainly caused by the low resolution of the inclinometer that I am using. A clear improvement is to use an inclinometer that has a higher resolution (eg. 1 decimal place). However, another approach is attempting to measure the length of the horizontal and vertical component of the frisbee, and use trigonometry to find θ, as shown in Figure 6.1 below.

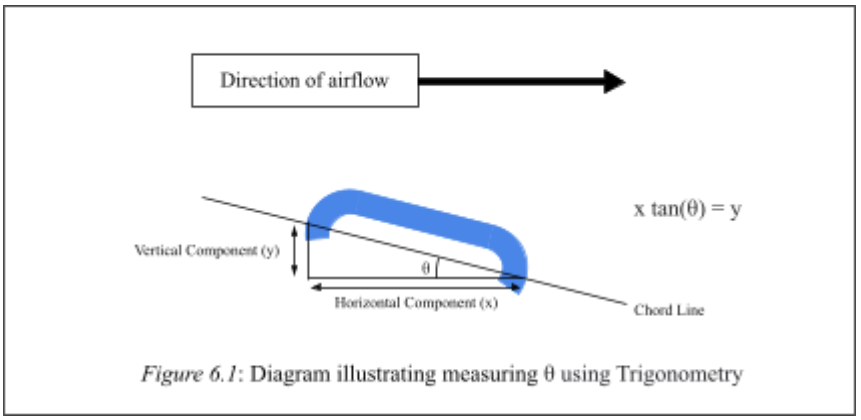

Figure 6.1: Diagram illustrating measuring θ using Trigonometry

6.3.2. Systematic Error

1. $1°$ ***on the Inclinometer may be smaller than that of the true value:***

This is most likely caused by miscalibration during manufacture. If no zero error is present, then C_L $(0°)$ will be unaffected, while causing the absolute value of θ to be greater than it actually is. Therefore, for C_L $(18°)$, this means that the measured F is for a smaller positive angle, meaning a smaller F, resulting in a smaller calculated value of C_L $(18°)$.

A possible improvement is, again, to use the trigonometry method as mentioned in Random Error 3 (assuming no zero error) as horizontal component is measured by calibrating 0°, therefore unaffected by miscalibration.

2. Assuming Dry Air:

As stated previously in 3. Variables and Preliminary Data, this accounts for at most 0.898% of discrepancy in the calculation of air density. As water has a smaller relative atomic mass than air, it means that dry air has a higher air density than moist air, meaning that the literature value of ρ is smaller than the calculated value. This causes the calculated C_L to be smaller than its true value.

The most feasible improvement to this is to measure the humidity of the environment and take it into account when calculating the specific gas constant of humid air at a certain humidity percentage.

3. Airflow created may not be Perfectly Laminar:

Despite using a wind tunnel to replicate laminar flow, turbulent airflow may still occur due to imperfections. As velocity of airflow v increases, the turbulence of air increases *(Mahrt, et al., 2014)*. In a research paper by *Yap, et al. (2001)*, the general observation for aerofoil NACA-0015 is that for

angle of attack smaller than the stalling angle, turbulence and C_L has a positive correlation, but as turbulence increases, the aerofoil stalls at a smaller angle.

For a frisbee disc, no stalling effect is observed between θ and F for $0° < \theta < 20°$ *(Figure 5.2)*. Hence, using *Mahrt, et al.(2014)* and *Yap, et al.(2001)*, it can be reasonably inferred that increase in turbulence causes measured C_L to be larger than the true value in that angle range.

The implication of a varying constant C_L is that the calculated gradient of v^2 and F in *Figure 5.1* would be larger than the true value. The y-intercept of the line of best fit would also deviate from the true value (the origin) as a result, which can be observed in *Figure 5.1*.

The most feasible improvement to this is to install honeycomb-shaped wire meshes and anti-turbulence screens in the wind tunnel to remove large vortexes and thus reduce turbulence *(Dehghan Manshadi, 2011)*.

6.4. Potential Further Investigation:

6.4.1. Investigating the stalling angle of a frisbee for $\theta > 0°$.

Stalling occurs due to an aerofoil's angle of attack becoming too large and disrupts laminar flow, causing turbulence. If this is the case, then it would be desirable to find out if there is a "maximum" and "minimum" lift force that acts on a frisbee, which I was unable to find out.

6.4.2. Investigating Drag of a frisbee in conjunction with lift, Investigating the Angle that gives the Highest Lift-to-Drag Ratio

Although lift is important to the flight of a frisbee, so is drag. If drag is too large, no matter how big the lift on the frisbee is, the frisbee will not travel far. If investigated together, it may give a deeper insight on how to optimally throw a frisbee. Furthermore, much like the Lift Equation, there is a Drag Equation ($F = - C_D \times A \times \frac{1}{2}\rho \times v^2$). They are nearly identical, except that the Coefficient of Drag (C_D) replaces C_L in the Drag Equation and that F is negative. This makes it desirable to investigate lift and drag together.

7. References

References

Air - Humidity ratio. (n.d.). The Engineering ToolBox. Retrieved November 7, 2022, from https://www.engineeringtoolbox.com/humidity-ratio-air-d_686.html

Air density calculator. (2017, May 10). Omni Calculator. https://www.omnicalculator.com/physics/air-density

Air density. (n.d.). NASA Glenn Research Center. Retrieved November 7, 2022, from https://www.grc.nasa.gov/www/k-12/VirtualAero/BottleRocket/airplane/fluden.html

Airfoil. (n.d.). U.S. Centennial of Flight. https://www.centennialofflight.net/essay/Dictionary/airfoil/DI2.htm

Angle of attack (AOA). (n.d.). SKYbrary Aviation Safety. https://skybrary.aero/articles/angle-attack-aoa

Approximate force on spinning ball. (n.d.). NASA Glenn Research Center. https://www.grc.nasa.gov/www/k-12/VirtualAero/BottleRocket/airplane/beach.html

Baumback, K. (2013). The aerodynamics of frisbee flight. *Undergraduate Journal of Mathematical Modeling: One + Two*, *3*(1). https://doi.org/10.5038/2326-3652.3.1.31

Bernoulli and Newton. (2022, July 27). Glenn Research Center | NASA. https://www1.grc.nasa.gov/beginners-guide-to-aeronautics/bernoulli-and-newton/

Bernoulli's equation. (2021, May 13). NASA Glenn Research Center. https://www.grc.nasa.gov/www/k-12/airplane/bern.html

Bernoulli's principle. (2020, December 10). BYJUS. https://byjus.com/physics/bernoullis-principle/

CK12-Foundation. (n.d.). CK-12 Foundation. https://flexbooks.ck12.org/cbook/ck-12-middle-school-earth-science-flexbook-2.0/section/10.3/primary/lesson/pressure-and-density-of-the-atmosphere-ms-es/

Continuity equation. (n.d.). Princeton University. https://www.princeton.edu/~asmits/Bicycle_web/continuity.html

Density_of_air. (n.d.). chemeurope.com - The chemistry information portal from laboratory to process. https://www.chemeurope.com/en/encyclopedia/Density_of_air.html

Discs & targets. (2022, September 30). WFDF. https://wfdf.sport/discs-targets/

Effect of size on lift. (2022, July 28). Glenn Research Center | NASA. https://www1.grc.nasa.gov/beginners-guide-to-aeronautics/effect-of-size-on-lift/

The four forces of flight. (n.d.). NASA. https://www.nasa.gov/audience/foreducators/k-4/features/F_Four_Forces_of_Flight.html

Hnidka, J., & Rozehnal, D. (2019). Calculation of the maximum endurance of a small unmanned aerial vehicle in a Hover. *IOP Conference Series: Materials Science and Engineering*, *664*(1), 012002. https://doi.org/10.1088/1757-899x/664/1/012002

Hummel, S. A., & Hubbard, M. (2019). Identification of Frisbee aerodynamic coefficients using flight data. https://silo.tips/download/identification-of-frisbee-aerodynamic-coefficients-using-flight-data

Labidi, A. (2019). What Is the Mach number? *Journal of Aviation/Aerospace Education & Research (JAAER)*. : https://www.researchgate.net/publication/337632133

Landell-Mills, N. (2019). Why lift quadruples if aircraft velocity doubles. https://doi.org/10.13140/RG.2.2.20536.70409

Landell-Mills, N. (2020). Newtons laws explain how frisbees fly. *European Journal of Applied Physics*, *2*(4). https://doi.org/10.24018/ejphysics.2020.2.4.9

Lift equation of the 1900's. (2021, May 10). Re-Living the Wright Way -- NASA. Retrieved November 7, 2022, from https://wright.grc.nasa.gov/airplane/liftold.html

Lift equation. (2022, July 28). Glenn Research Center | NASA. https://www1.grc.nasa.gov/beginners-guide-to-aeronautics/lift-equation/

Lissaman, P., & Hubbard, M. (2010). Maximum range of flying discs. *Procedia Engineering*, *2*(2), 2529-2535. https://10.1016/j.proeng.2010.04.027

Mahrt, L. (2014). Dependence of Turbulent Velocities on Wind Speed and Stratification. https://link.springer.com/content/pdf/10.1007/s10546-014-9992-5.pdf

Mass flow rate. (2022, July 21). Glenn Research Center | NASA. https://www1.grc.nasa.gov/beginners-guide-to-aeronautics/mass-flow-rate/

Modern lift equation. (2021, May 10). Re-Living the Wright Way -- NASA. Retrieved November 7, 2022, from https://wright.grc.nasa.gov/airplane/lifteq.html

Morrison, V. R. (2005). The Physics of Frisbees.

Nave, R. (n.d.). *Airfoils, Bernoulli and Newton*. https://hyperphysics.phy-astr.gsu.edu/hbase/Fluids/airfoil.html

Nave, R. (n.d.). *Pressure*. https://hyperphysics.phy-astr.gsu.edu/hbase/pber.html#beq

Newton's laws of motion. (2022, October 27). Glenn Research Center | NASA. https://www1.grc.nasa.gov/beginners-guide-to-aeronautics/newtons-laws-of-motion/

Physics of a frisbee – the ultimate way of throwing a frisbee. (2017, October 7). The University of Melbourne. https://blogs.unimelb.edu.au/sciencecommunication/2017/10/07/physics-of-a-frisbee-the-ultimate-way-of-throwing-a-frisbee/

Potts, J. (2005). Disc-wing Aerodynamics.

Potts, J., & Crowther, W. (2002). Frisbee(TM) aerodynamics. *20th AIAA Applied Aerodynamics Conference*. https://doi.org/10.2514/6.2002-3150

Potts, J., & Crowther, W. J. (2005). Comparison of the present experimental data to Frisbee-like circular planform wings from the literature - Lift Coefficient [Graph]. https://www.researchgate.net/publication/268559957_FrisbeeTM_Aerodynamics

Scodary, A. (2007, October 30). *The Aerodynamics and Stability of Flying Discs*. The Aerodynamics and Stability of Flying Discs. Retrieved November 7, 2022, from http://large.stanford.edu/courses/2007/ph210/scodary1/

Smeaton pressure coefficient. (2021, May 10). Re-Living the Wright Way -- NASA. Retrieved November 7, 2022, from https://wright.grc.nasa.gov/airplane/smeaton.html

Stall. (n.d.). SKYbrary Aviation Safety. https://skybrary.aero/articles/stall

Student airfoil interactive. (2022, September 16). Glenn Research Center | NASA. https://www1.grc.nasa.gov/beginners-guide-to-aeronautics/foilsimstudent/

Sumaryada, T., Jaya, A. M., & Kartono, A. (2018). Simulating the Aerodynamics Profiles of NACA 4312 Airfoil in Various Incoming Airspeed and Gurney Flap Angle.

Theory of flight. (1997, March 16). MIT - Massachusetts Institute of Technology. Retrieved November 7, 2022, from https://web.mit.edu/16.00/www/aec/flight.html

Velocity effects on aerodynamic forces. (2021, May 13). NASA Glenn Research Center. Retrieved November 7, 2022, from https://www.grc.nasa.gov/www/k-12/rocket/vel.html

What is lift? (2022, July 21). Glenn Research Center | NASA. https://www1.grc.nasa.gov/beginners-guide-to-aeronautics/what-is-lift/

Wing geometry definitions interactive. (2022, July 21). Glenn Research Center | NASA. https://www1.grc.nasa.gov/beginners-guide-to-aeronautics/wing-geometry-interactive/

Wings and lift. (n.d.). Science Learning Hub. https://www.sciencelearn.org.nz/resources/300-wings-and-lift

Yap, T. C., Abdullah, M. Z., Husain, Z., Ripin, M., & Ahmad, R. (2001). THE EFFECT OF TURBULENCE INTENSITY ON THE AERODYNAMIC PERFORMANCE OF AIRFOILS. https://www.researchgate.net/publication/268524113_THE_EFFECT_OF_TURBULENCE_INTENSITY_ON_THE_AERODYNAMIC_PERFORMANCE_OF_AIRFOILS

8. Appendices

Appendix A: Calculations for Percentage Discrepancy between the Specific Gas Constant of Dry Air and Humid Air at 298.0 K.

Relative Atomic Mass of Dry Air ($M_r: dry\ air$) $= 28.97\ gmol^{-1}$**(2dp)**

Relative Atomic Mass of Water ($M_r: H_2O$) $= 18.02\ gmol^{-1}$(2dp)

Air-to-water mass ratio of 100% humid air $= 1: 0.019826$

Relative Atomic Mass of 100% Humid Air ($M_r: humid\ air$) $= \frac{1 \times 28.97\ gmol^{-1} + 0.019826 \times 18.02\ gmol^{-1}}{1 + 0.019826}$

$= 28.76\ gmol^{-1}$**(2dp)**

Percentage Discrepancy of $M_r: dry\ air$ from $M_r: humid\ air$ $= \frac{28.97 gmol^{-1} - 28.76\ gmol^{-1}}{28.76\ gmol^{-1}} \times 100\%$

$= 0.730\%$ **(3sf)**.

Appendix B: Raw Data for How Velocity of Airflow affects Lift Force generated by a Frisbee for Velocity Lift Frisbee Experiment

Wind Speed, v/ms^{-1}						Uncertainty of v/ms^{-1}	% Uncertainty of v	v^2/m^2s^{-2}	% Uncertainty of v^2	Uncertainty of v^2/m^2s^{-2}
Trial 1	Trial 2	Trial 3	Trial 4	Trial 5	Average					
4.20	4.27	4.20	4.13	4.13	4.19	0.07	1.60	17.36	3.20	0.56
3.67	3.57	3.70	3.67	3.80	3.68	0.12	3.15	13.69	6.31	0.86
3.33	3.33	3.30	3.37	3.33	3.33	0.03	1.00	11.11	2.00	0.22
2.43	2.37	2.50	2.50	2.47	2.45	0.07	2.70	6.08	5.41	0.33
3.00	2.97	2.93	3.07	3.03	3.00	0.07	2.22	9.00	4.44	0.40
4.00	4.07	3.97	3.93	4.07	4.01	0.07	1.67	16.00	3.33	0.53
1.97	1.90	2.00	1.97	1.97	1.96	0.05	2.54	3.87	5.08	0.20

Mass Recorded on Weighing Scale, $m/g + 2400.00g$														
Trial 1					Trial 2					Trial 3				
7.90	5.42	4.39	6.75	5.32	6.55	7.52	6.52	7.82	9.71	3.02	4.40	4.78	5.69	5.78
13.54	14.05	16.91	17.30	16.60	16.63	17.29	15.66	14.35	14.99	15.13	14.10	14.72	16.67	15.21
21.05	22.66	21.31	22.40	23.61	20.54	21.92	22.25	23.11	20.89	23.87	21.10	21.72	21.38	21.29
29.70	29.12	28.32	29.19	29.35	28.91	27.85	28.28	28.01	31.20	27.78	27.71	28.26	26.69	27.21
23.88	22.00	27.35	26.10	25.73	27.22	25.36	27.83	23.93	25.09	24.89	25.25	27.56	24.02	24.40
13.44	11.11	9.78	10.76	8.38	9.82	9.84	9.54	10.89	10.31	7.37	7.15	10.95	10.04	8.42
35.78	26.15	36.89	35.25	37.26	39.33	40.16	39.22	39.47	35.51	35.93	37.42	38.96	38.21	39.98

Mass Recorded on Weighing Scale, $m/g + 2400.00g$												
Trial 4					Trial 5					$1st$ Quartile	$3rd$ Quartile	Interquartile Mean
4.16	5.21	7.14	6.99	7.83	6.57	5.64	6.34	6.61	6.77	5.32	6.99	5.44
15.40	15.13	16.68	18.73	16.50	15.85	16.08	15.43	15.92	13.34	14.99	16.63	15.73
21.17	20.54	22.59	22.09	22.69	22.96	24.09	22.48	20.88	22.46	21.17	22.66	21.98
31.03	31.54	31.63	32.16	30.70	31.57	30.51	32.22	32.89	33.14	28.26	31.54	29.70
24.43	23.13	22.63	24.87	24.58	23.84	25.60	23.81	24.98	24.96	23.93	25.60	24.80
10.40	9.38	10.66	9.35	10.02	8.77	7.74	11.38	10.96	11.93	9.35	10.89	9.67
41.17	41.00	41.61	41.05	37.59	36.57	35.72	29.43	31.31	30.58	35.72	39.47	37.57

Change in Mass after Airflow, $\Delta m/g$	Lift Force Generated by Frisbee, F/N	Uncertainty of $\Delta m/g$	% Uncertainty of Δm, % Uncertainty of F	Uncertainty of F/N
-37.14	0.364	0.835	2.25	0.008
-26.85	0.263	0.820	3.05	0.008
-20.60	0.202	0.745	3.62	0.007
-12.88	0.126	1.640	12.7	0.016
-17.78	0.174	0.835	4.70	0.008
-32.91	0.323	0.770	2.34	0.008
-5.01	0.049	1.875	37.4	0.018

Appendix C: Raw Data for How Angle of Attack affects Lift Force generated by a Frisbee for Angle of Attack Lift Frisbee Experiment

Angle of Attack, $\theta/° \pm 0.5°$	% Uncertainty of θ	Mass Recorded on Weighing Scale, $m/g + 2400.00g$									
		Trial 1					Trial 2				
-18.0	2.78	51.42	52.23	52.57	53.73	52.15	52.42	53.43	53.36	53.32	53.20
-16.0	3.13	49.14	50.46	50.22	50.52	50.82	51.78	51.02	51.41	51.11	51.35
-14.0	3.57	50.64	50.19	49.13	51.60	49.08	49.58	49.63	50.36	49.53	50.65
-12.0	4.17	47.94	50.54	47.72	49.32	46.82	49.07	49.76	49.49	46.86	49.08
-10.0	5.00	46.01	46.53	47.51	46.33	46.28	44.13	46.09	45.14	46.51	47.30
-8.0	6.25	45.53	45.67	43.83	45.85	43.85	45.15	45.70	48.29	46.27	44.54
-6.0	8.33	43.08	40.17	44.17	39.82	41.61	43.02	40.90	44.44	43.88	44.98
-4.0	12.5	39.75	37.71	36.18	39.98	39.67	41.43	39.27	40.25	40.76	39.01
-2.0	25.0	38.00	36.58	37.22	37.77	38.12	40.77	37.97	38.69	36.66	37.97
0.0	-	37.93	40.21	35.74	34.71	36.78	32.60	32.96	35.37	35.32	36.39
2.0	25.0	31.21	31.99	31.75	31.92	31.99	31.77	34.03	35.41	32.12	33.83
4.0	12.5	31.06	27.68	28.65	27.37	29.27	30.09	30.69	29.91	29.65	31.83
6.0	8.33	26.25	25.49	23.73	26.56	25.45	27.44	28.93	29.23	25.69	26.78
8.0	6.25	23.64	22.65	22.86	24.56	21.86	23.86	22.33	23.37	23.72	23.77
10.0	5.00	21.33	22.01	20.02	19.97	20.60	21.81	22.12	20.35	20.93	20.26
12.0	4.17	16.97	16.80	17.52	17.97	16.26	18.45	16.50	18.10	19.95	18.74
14.0	3.57	13.84	15.39	13.04	15.38	13.49	15.80	15.90	16.16	15.41	15.67
16.0	3.13	8.81	7.83	8.62	9.28	8.00	14.55	11.36	11.72	11.99	13.28
18.0	2.78	8.20	8.02	10.45	8.94	8.17	7.95	10.13	9.86	10.28	9.26

Mass Recorded on Weighing Scale, $m/g + 2400.00g$														
Trial 3					Trial 4					Trial 5				
51.75	50.78	52.32	53.90	52.25	50.71	52.39	51.79	51.65	52.10	55.56	55.07	55.34	55.26	54.66
51.28	51.57	51.02	50.23	51.09	51.48	51.60	51.59	52.16	52.17	51.45	52.70	55.03	51.56	52.10
50.65	50.80	49.70	49.34	48.83	51.91	50.82	51.07	50.28	50.46	54.72	51.72	52.13	51.23	52.18
47.81	48.05	47.28	49.50	48.07	45.51	49.58	49.47	48.57	48.41	51.63	49.17	53.00	52.40	50.91
43.88	45.70	45.12	46.67	44.92	44.64	48.12	49.84	45.59	45.61	46.85	48.39	49.03	48.66	47.72
46.22	44.65	43.61	45.00	43.13	46.12	45.77	45.05	46.16	45.63	46.50	48.28	44.42	46.29	46.00
42.42	45.36	43.29	41.04	41.40	41.44	42.18	43.16	42.92	42.94	41.49	44.28	44.03	45.56	45.33
41.75	42.06	41.32	40.95	41.08	39.98	41.04	40.00	41.73	40.87	42.95	43.58	45.23	43.16	42.68
38.93	37.97	37.46	36.66	38.58	37.68	39.03	39.06	39.33	38.66	38.13	39.61	39.01	41.57	37.65
35.89	38.28	36.90	36.79	34.86	35.58	36.63	35.34	35.83	36.70	35.87	37.93	37.14	36.93	34.18
35.10	32.48	33.49	33.38	35.87	32.97	33.08	34.39	33.67	34.30	37.35	36.06	32.89	33.36	35.26
32.26	32.39	31.99	29.31	30.24	32.20	31.01	27.81	30.05	29.77	33.44	32.02	32.25	32.21	31.21
29.73	28.24	29.08	26.02	26.84	30.76	30.93	29.16	31.11	30.73	25.37	25.59	29.77	28.17	28.22
25.70	26.32	25.24	24.97	25.46	25.92	23.78	27.16	25.24	24.85	24.49	25.62	27.48	27.74	28.32
24.55	24.40	21.82	23.48	21.77	22.13	24.45	22.35	24.95	18.81	24.27	22.12	21.30	25.15	22.57
19.85	22.03	21.04	21.24	20.99	20.71	21.84	21.63	22.22	21.33	18.81	18.05	15.30	18.46	20.34
17.40	18.19	17.80	18.29	18.20	16.35	17.80	20.55	20.43	19.02	16.43	18.45	17.45	21.14	19.28
14.51	11.75	14.11	16.27	15.46	17.75	16.30	13.29	13.62	12.72	13.75	10.54	13.04	13.32	11.60
13.28	11.65	11.43	10.85	13.13	14.08	12.21	11.55	7.86	8.76	7.72	8.30	8.76	11.01	11.52

Mass Recorded on Weighing Scale, $m/g + 2400.00g$			Change in Mass after Airflow, $\Delta m/g$	Lift Force Generated by Frisbee, F/N	Uncertainty of $\Delta m/g$	% Uncertainty of Δm and F	Uncertainty of F/N
$1st$ Quartile	$3rd$ Quartile	Interquartile Mean					
52.10	53.73	52.73	10.31	-0.101	0.815	7.91	0.008
51.02	51.60	51.35	8.93	-0.088	0.290	3.25	0.003
49.63	51.23	50.50	8.08	-0.079	0.800	9.90	0.008
47.94	49.58	48.90	6.48	-0.064	0.820	12.7	0.008
45.59	47.51	46.38	3.96	-0.039	0.960	24.2	0.009
44.65	46.16	45.56	3.14	-0.031	0.755	24.0	0.007
41.49	44.17	42.94	0.52	-0.005	1.340	259	0.013
39.98	41.75	40.86	-1.56	0.015	0.885	56.6	0.009
37.68	39.01	38.27	-4.15	0.041	0.665	16.0	0.007
35.34	36.90	36.14	-6.28	0.062	0.780	12.4	0.008
32.12	34.39	33.38	-9.04	0.089	1.135	12.6	0.011
29.65	32.02	30.73	-11.69	0.115	1.185	10.1	0.012
26.02	29.23	27.76	-14.66	0.144	1.605	11.0	0.016
23.72	25.70	24.71	-17.71	0.174	0.990	5.59	0.010
20.93	23.48	21.98	-20.44	0.201	1.275	6.24	0.013
17.97	21.04	19.34	-23.08	0.226	1.535	6.65	0.015
15.67	18.29	17.03	-25.39	0.249	1.310	5.16	0.013
11.36	14.11	12.62	-29.80	0.292	1.375	4.61	0.013
8.30	11.52	9.47	-32.95	0.323	1.610	4.89	0.016

Appendix D: Derivation of Multivariable Regression of v^2 and θ against F.

$f(v^2) = 0.02193v^2 - 0.02658.$

$g(\theta) = \begin{cases} 0.01412\,\theta + 0.06561, -1 < \theta \leq 18 \\ 0.000237\,\theta^2 + 0.01356\,\theta + 0.06655, -18 \leq \theta \leq -1 \end{cases}.$

$f(v^2)$ is a function that measures F when $\theta = 18°$. $g(\theta)$ is a function that measures F when $v^2 = 16.0\ m^2 s^{-2}$.This means that by definition, when $f(v^2) = 0$ or $g(\theta) = 0$, $F = 0$. Therefore, it can be deduced that:

$$F = k \times f(v^2) \times g(\theta) \text{ [8.0.1]},$$

where k is a constant to be determined.

As shown in both *Table 2* and *Table 4*, for $v^2 = 16.0 m^2 s^{-2}$ and $\theta = 18°$, $F = 0.323\ N$. Therefore, it can be stated that:

$$0.323 = k \times f(16.0) \times g(18) \text{ [8.0.2]}$$

$$0.323 = k \times (0.02193 \times (16.0) - 0.02658) \times (0.01412 \times (18) + 0.06561) \text{ [8.0.3]}$$

$$0.323 = k \times 0.1037 \text{ [8.0.4]}$$

$$\frac{0.323}{0.1037} = k \text{ [8.0.3]}$$

$$k = 3.11 \text{ [8.0.3]}$$

Hence, by substituting $k = 3.11$ into [8.0.1], the variables of θ, v^2 and F can be related using the multivariable regression:

$$F = 3.11 \times f(v^2) \times g(\theta) \text{ [8]}.$$

Appendix E: Code used to graph the 3D Regression plotted in *Figure 5.3* using Python.

```
from mpl_toolkits.mplot3d import axes3d
import matplotlib.pyplot as plt
from matplotlib import style
import numpy as np

fig = plt.figure()
plt.style.use('default')

ax = fig.add_subplot(111, projection='3d')
plt.title("Figure 5.3: 3D Regression of Square of Velocity, Angle of Attack, and
Lift Force using Figure 5.1 and 5.2")

ax.set_xlabel('Square of Velocity/m^2s^-2')
ax.set_ylabel('Angle of Attack/°')
ax.set_zlabel('Lift Force/N')
# actual surface
for count in range(-10, 181):
    x1 = np.linspace(0, 20, 20)

    y1 = np.linspace(count / 10, count / 10, 20)

    z1 = 3.11 * (0.02193 * x1 - 0.02658) * (0.01412 * y1 + 0.06561)

    if count % 50 == 0:
        ax.plot(x1, y1, z1, color="white", alpha=1)
    else:
        ax.plot(x1, y1, z1, color="blue", alpha=0.3)

for count in range(0, 20):
    if count % 5 == 0:
        x1 = np.linspace(count, count, 20)

        y1 = np.linspace(-1, 18, 20)

        z1 = 3.11 * (0.02193 * x1 - 0.02658) * (0.01412 * y1 + 0.06561)
        ax.plot(x1, y1, z1, color="white", alpha=1)

for count in range(-180, -10):
    x1 = np.linspace(0, 20, 20)

    y1 = np.linspace(count / 10, count / 10, 20)
```

```
    z1 = 3.11 * (0.02193 * x1 - 0.02658) * (0.000237 * y1 ** 2 + 0.01356 * y1 +
0.06655)

    if count % 50 == 0:
        ax.plot(x1, y1, z1, color="white", alpha=1)
    else:
        ax.plot(x1, y1, z1, color="blue", alpha=0.3)

for count in range(0, 20):
    if count % 5 == 0:
        x1 = np.linspace(count, count, 20)

        y1 = np.linspace(-18, -1, 20)

        z1 = 3.11 * (0.02193 * x1 - 0.02658) * (0.000237 * y1 ** 2 + 0.01356 * y1
+ 0.06655)
        ax.plot(x1, y1, z1, color="white", alpha=1)

# x = 20
for count in range(-90, -5):
    x1 = 20
    x2 = np.linspace(x1, x1, 20)

    y1 = count/5
    y2 = np.linspace(y1, y1, 20)

    z2 = np.linspace(0, 3.11 * (0.02193 * x1 - 0.02658) * (0.000237 * y1 ** 2 +
0.01356 * y1 + 0.06655), 20)

    if count % 25 == 0:
        ax.plot(x2, y2, z2, color="white", alpha=0.3)
    else:
        ax.plot(x2, y2, z2, color="blue", alpha=0.2)

for count in range(-5, 90):
    x1 = 20
    x2 = np.linspace(x1, x1, 20)

    y1 = count/5
    y2 = np.linspace(y1, y1, 20)

    z2 = np.linspace(0, 3.11 * (0.02193 * x1 - 0.02658) * (0.01412 * y1 +
0.06561), 20)
    if count % 25 == 0:
        ax.plot(x2, y2, z2, color="white", alpha=0.3)
    else:
        ax.plot(x2, y2, z2, color="blue", alpha=0.2)
```

```
# y = 18
for count in range(0, 200):
    x1 = count/10
    x2 = np.linspace(x1, x1, 20)

    y1 = 18
    y2 = np.linspace(y1, y1, 20)

    z2 = np.linspace(0, 3.11 * (0.02193 * x1 - 0.02658) * (0.01412 * y1 +
0.06561), 20)

    if count % 50 == 0:
        ax.plot(x2, y2, z2, color="white", alpha=0.3)
    else:
        ax.plot(x2, y2, z2, color="blue", alpha=0.2)

# y = -18
for count in range(0, 200):
    x1 = count/10
    x2 = np.linspace(x1, x1, 20)

    y1 = -18
    y2 = np.linspace(y1, y1, 20)

    z2 = np.linspace(0, 3.11 * (0.02193 * x1 - 0.02658) * (0.000237 * y1 ** 2 +
0.01356 * y1 + 0.06655), 20)

    if count % 50 == 0:
        ax.plot(x2, y2, z2, color="white", alpha=0.3)
    else:
        ax.plot(x2, y2, z2, color="blue", alpha=0.2)

# z = 0
for count in range(0, 100):
    x2 = np.linspace(count/5, count/5, 20)

    y2 = np.linspace(-18, 18, 20)

    z2 = np.linspace(0, 0, 20)

    ax.plot(x2, y2, z2, color="black", alpha=0.5)

ax.set_xlim3d(0, 20)
ax.set_ylim3d(-18, 18)
```

```
ax.set_zlim3d(-0.2, 0.5)

# plot data point for theta and f
v = np.linspace(16, 16, 19)

theta = [-18.0,
-16.0,
-14.0,
-12.0,
-10.0,
-8.0,
-6.0,
-4.0,
-2.0,
0.0,
2.0,
4.0,
6.0,
8.0,
10.0,
12.0,
14.0,
16.0,
18.0,]

F = [-0.101,
-0.088,
-0.079,
-0.064,
-0.039,
-0.031,
-0.005,
0.015,
0.041,
0.062,
0.089,
0.115,
0.144,
0.174,
0.201,
0.226,
0.249,
0.292,
0.323]
for count in range(0,19):
    ax.plot(v[count], theta[count], F[count], color="orange", alpha=1,
marker="x")
```

```
v = [17.36,
13.69,
11.11,
6.08,
9.00,
16.00,
3.87]

theta = np.linspace(18, 18, 7)

F = [0.364,
0.263,
0.202,
0.126,
0.174,
0.323,
0.049]

for count in range(0,7):
    ax.plot(v[count], theta[count], F[count], color="orange", alpha=1,
marker="x")

plt.show()
```